



## Arrangement and electronic properties of cobalt phthalocyanine molecules on B-Si(111)- $\sqrt{3} \times \sqrt{3} R30^\circ$

Susi Lindner,<sup>\*</sup> Martin Franz , Milan Kubicki, Stephan Appelfeller, Mario Dähne, and Holger Eisele  
*Institut für Festkörperphysik, Technische Universität Berlin, Hardenbergstraße 36, 10623 Berlin, Germany*

 (Received 25 September 2019; published 4 December 2019)

The molecular arrangement and the interfacial electronic properties of cobalt phthalocyanine (CoPc) on the deactivated B-Si(111)- $\sqrt{3} \times \sqrt{3} R30^\circ$  surface are analyzed using scanning tunneling microscopy and spectroscopy as well as photoemission studies. Our data demonstrate that for low coverages of CoPc the molecules lie flat with the  $p_z$  orbital of the Si surface atom forming a hybrid state with the  $d_{z^2}$  orbital of the transition metal. This hybridization is observed in a broadening of the corresponding Si  $2p$  core level photoemission spectra and in an additional contribution to the valence band spectra. Furthermore, this additional hybridization state is detected in the tunneling spectra. For higher CoPc coverages, the CoPc molecules are tilted with respect to the Si surface forming highly ordered organic molecular films. The spectroscopic data of the thick film demonstrates that the electronic properties resemble those of pure CoPc.

DOI: [10.1103/PhysRevB.100.245301](https://doi.org/10.1103/PhysRevB.100.245301)

### I. INTRODUCTION

The formation of self-assembled monolayers of organic molecular materials on solid surfaces is an important subject, both from the viewpoint of fundamental science and in regard of applications. In particular, the understanding of various phenomena and processes that can occur at the interfaces between organic films and solid substrates is crucial for the performance of devices based on organic materials. Thus, research on organic thin films has intensified in recent years because of their possible applications in advanced optical and electronic devices.

Transition metal phthalocyanines (TMPc) represent a family of organic semiconductors, which are based on a  $\pi$ -conjugated macrocycle ring. The structure is shown in Fig. 1(a) for the case of Co as transition metal. TMPc are widely investigated and have been used already in organic light-emitting diodes [1], organic photovoltaic cells [1–3], organic field-effect transistors [4], and organic spintronic devices [5,6]. The performance of TMPc in such devices is strongly affected by interface interactions, which can be adjusted both in strength and in nature by choosing specific substrates. TMPc have a planar structure with a  $D_{4h}$  symmetry. The five transition metal  $3d$  orbitals transform as  $a_{1g}$  ( $d_{z^2}$ ),  $b_{1g}$  ( $d_{x^2-y^2}$ ),  $e_g$  ( $d_{xz}$ ,  $d_{yz}$ ), and  $b_{2g}$  ( $d_{xy}$ ). For cobalt phthalocyanine (CoPc) with a  $d^7$  configuration and  $S = 1/2$ , the ground state is  $b_{1g}^0 a_{1g}^1 e_g^4 b_{1g}^2$ . Due to its partially filled  $d_{z^2}$  orbital, CoPc is an interesting candidate for interface research.

At this time, many studies of CoPc on metal surfaces exist, for example, CoPc on Ag(111) [7–9], on Cu(111) [10], and on Au [11–13]. However, the combination of transition metal phthalocyanines with the existing microelectronics technology, being predominantly silicon based, has the potential of novel applications in semiconductor devices. Moreover, in contrast

to metals, semiconductor substrates offer the possibility to tune the molecule-substrate interaction by a passivation of the surface.

A prominent example in this case is the B-Si(111)- $\sqrt{3} \times \sqrt{3} R30^\circ$  (Si:B) surface [14–16]. A model of this surface is depicted in Fig. 1(b). The incorporation of B atoms in the subsurface layer leads to a removal of the dangling bonds of the Si(111) surface [17,18]. This results in an empty  $p_z$  orbital of the Si adatom and a chemical deactivation of the surface. Recently, it was shown that an interface between CoPc and Si:B is characterized by an interface charge transfer [19]. This is in contrast to ZnPc on Si:B, for which no charge transfer occurs due to the fully filled  $d$  orbitals of the Zn atoms [20].

In this contribution we study the molecular arrangement and the electronic properties of CoPc on the deactivated Si:B surface in detail by means of scanning tunneling microscopy (STM) as well as spectroscopy (STS). Our data clearly demonstrate that submonolayers of CoPc lie flat on the surface and that a selective orbital hybridization occurs. Furthermore, our photoemission spectroscopy (PES) data support the model of the formation of a local hybrid state between the partially filled  $d_{z^2}$  orbital of the CoPc molecule and the empty  $p_z$  orbital of the Si adatom. For high CoPc coverages, in contrast, CoPc molecules are tilted with respect to the Si:B surface, establishing exceedingly ordered molecular arrangements. The spectroscopic data clearly show that several monolayers of CoPc feature identical electronic properties as pure CoPc.

### II. EXPERIMENT

Heavily  $p$ -doped Si(111) wafers (B doped,  $<0.002 \Omega \text{ cm}$ ) obtained from Crystec GmbH, Berlin, were used as substrates. They were *in situ* annealed repeatedly at  $1200^\circ \text{C}$  to remove the surface contamination, followed by an annealing step at  $900^\circ \text{C}$  for 30 min to induce the subsurface B segregation. This process results in an atomically smooth and passivated Si:B surface. The samples were heated by direct current and their

<sup>\*</sup>slindner@physik.tu-berlin.de

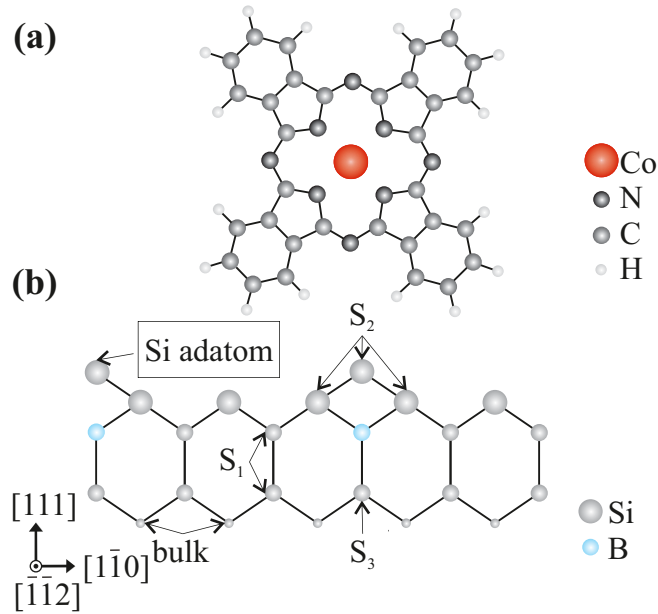


FIG. 1. (a) Structure of the cobalt phthalocyanine molecule (CoPc,  $\text{CoC}_{32}\text{N}_8\text{H}_{16}$ ) with the central atom ( $\text{Co}^{2+}$ ) being surrounded by the ligand ( $\text{C}_{32}\text{N}_8\text{H}_{16}^{2-}$ ). (b) Schematic side view of a B-Si(111)- $\sqrt{3} \times \sqrt{3}R30^\circ$  surface (Si:B). Additionally, the notation for the corresponding components in the Si  $2p$  core level spectra are marked by  $S_1$  to  $S_3$  and bulk.

temperature was monitored using an infrared pyrometer with an accuracy of  $\pm 20^\circ\text{C}$ .

CoPc molecules were deposited *in situ* by thermal evaporation onto the Si:B substrate kept at room temperature. The growth rate was controlled by using a quartz-crystal microbalance calibrated by determining the coverage from STM images measured for low CoPc coverages. A coverage of 1 monolayer (ML) is defined as an area completely covered by flat-lying CoPc molecules, i.e., a density of  $4 \times 10^{13}$  molecules/ $\text{cm}^2$ .

The STM experiments were performed *in situ* at room temperature using a noncommercial STM setup with a Nanonis SPM control system. The base pressure was lower than  $5 \times 10^{-11}$  mbar during the measurements. The tunneling tips were prepared by electrochemical etching of W wires and further cleaned *in situ* by electron bombardment. All STM images were acquired using the constant current mode.

STS spectra were taken at distinct points of the surface with the feedback loop turned off. Besides  $I$ - $V$  spectra,  $dI/dV$ - $V$  spectra were measured simultaneously using a software lock-in amplifier. For this purpose, the tunneling voltage was modulated with a frequency of 1 kHz and an amplitude of  $V_{\text{mod}} = 50$  mV. Since the measured  $dI/dV$  signal is rather small for small tunneling voltages, the normalized derivative  $(dI/dV)/(\bar{I}/\bar{V})$  was calculated, which should reasonably well represent the local density of states (LDOS) [21,22]. In order to prevent a division by zero within the energy gap, the normalization was performed similar to Ref. [23] replacing  $(\bar{I}/\bar{V})$  by  $\sqrt{(\bar{I}^2 + c^2)}/\bar{V}^2$ , with  $c$  being a small constant just above the noise level [24].

The photoelectron spectroscopy experiments have been carried out in normal emission geometry using a separate ultrahigh vacuum system, which is equipped with a PHOIBOS-100 electron-energy analyzer (SPECS). Photons were provided by the UE112 PGM-1 beamline at BESSY II.

### III. RESULTS AND DISCUSSION

In order to analyze the geometric arrangement of the CoPc molecules on the Si:B surface we start with an overview empty states STM image of 0.2 ML CoPc deposited onto a clean Si:B surface, shown in Fig. 2(a). In this case the CoPc molecules lie flat on the surface, so that the molecular planes are parallel to the Si surface. In Fig. 2(b) a detailed empty states STM image of a single flat-lying CoPc molecule is shown. The four benzene rings appear as bright protrusions, while the Co atom appears even brighter due to the orbital-mediated tunneling [19,25]. The adsorption site of the CoPc molecule is determined from a detailed analysis of the STM data: All molecules in the image in Fig. 2(a) [also visible in the magnified image in Fig. 2(b)] are located with respect to the surrounding Si:B lattice in a way that their center is found at the position of the Si adatom. Thus, the central Co atom lies directly above the Si adatom, which is depicted schematically in Fig. 2(c). Only in this molecular arrangement a strong interaction is possible, resulting in a hybridization of the singly occupied  $d_{z^2}$  orbital of the CoPc molecules and the empty  $p_z$  orbital of the Si adatom [19,26].

A closer inspection of Fig. 2(b) reveals that the orientation of the molecule is characterized by two molecule sides aligned along the  $(\bar{1}\bar{1}2)$  directions. Due to the fourfold symmetry of the molecules and the threefold symmetry of the substrate, this results in three different rotational configurations, as indicated in Fig. 2(a) by the differently colored squares.

For higher CoPc coverages, as shown in Fig. 3(a), domains with a tilted molecular configuration emerge on a long scale

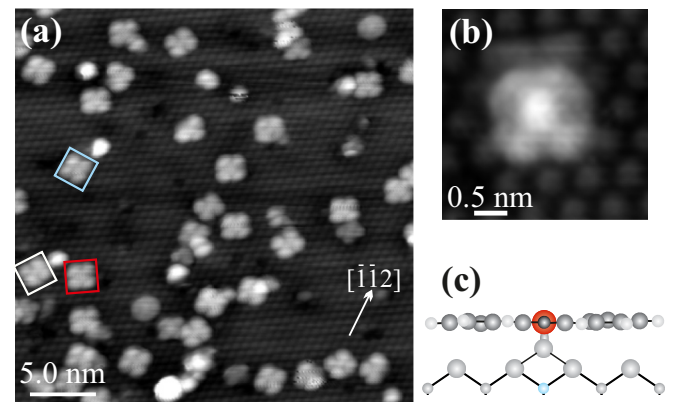


FIG. 2. (a) Overview empty states STM image of a passivated Si:B substrate with a CoPc coverage of 0.2 ML (sample voltage  $V_S = +1.8$  V, tunneling current  $I_T = 50$  pA). The different molecular orientations are indicated by colored squares. (b) Empty states STM image of a single flat-lying CoPc molecule ( $V_S = +2.0$  V,  $I_T = 20$  pA). (c) Schematic diagram of a single flat-lying CoPc molecule on Si:B (side view). The central Co atom lies directly above the Si:B adatom.

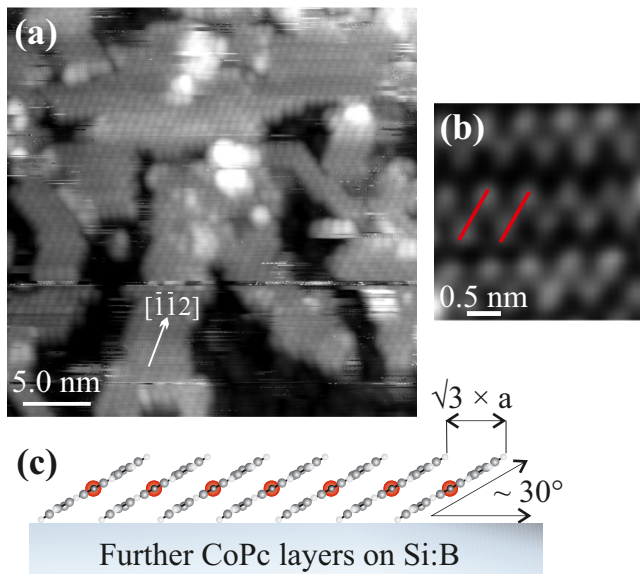


FIG. 3. (a) Overview empty states STM image of a Si:B surface with a CoPc coverage of 3.2 ML ( $V_S = +2.5$  V,  $I_T = 20$  pA). (b) Detailed empty states STM image of the typical tilted packing of CoPc molecules within a domain ( $V_S = +2.5$  V,  $I_T = 10$  pA). The red bars indicate the signal from the two upper benzene rings of individual molecules. (c) Schematic diagram of the molecular arrangement of tilted CoPc molecules lying on further CoPc layers on the deactivated Si:B surface.

range. This becomes evident in the detailed empty states STM image in Fig. 3(b), showing ordered chains of tilted CoPc molecules within a single domain. Here the typical parallel packing can be seen. In this tilted configuration, only the two upper benzene rings are observed for each CoPc molecule, appearing as bright protrusions. In contrast to the flat-lying configuration, the Co atom is not visible any more. A schematic diagram of the arrangement of tilted CoPc molecules on the deactivated Si:B surface is shown in Fig. 3(c).

In order to determine the apparent heights and the tilt angles of the molecules, height contours are presented in Fig. 4 for different CoPc coverages. For the ordered CoPc multilayer [Fig. 4(c)], the single molecular step amounts to 0.6 nm. Considering a width of a single CoPc molecule of 1.2 nm, similar to Ref. [27], a tilt angle of about  $30^\circ$  is determined. The same result is obtained for the monolayer [right side of the height profile in Fig. 4(b)], where again a step height of 0.6 nm from the substrate to the monolayer surface is found. In contrast to these thicker films, the CoPc submonolayer coverage, characterized by flat-lying molecules, only appears with heights around 0.25 nm, as shown in Fig. 4(a) and on the left side of the height profile of Fig. 4(b). Such ordered and tilted CoPc monolayer and multilayer films on Si:B are drastically different compared to the close-packed flat-lying CoPc molecules on many metals [13,28,29], while a tilted arrangement was also observed in the case of semiconductors or insulators [30–34].

In order to gain more insight into the nature of the molecule-substrate interaction and the charge transfer mechanisms, the Si  $2p$  core level PES spectra of the clean Si:B

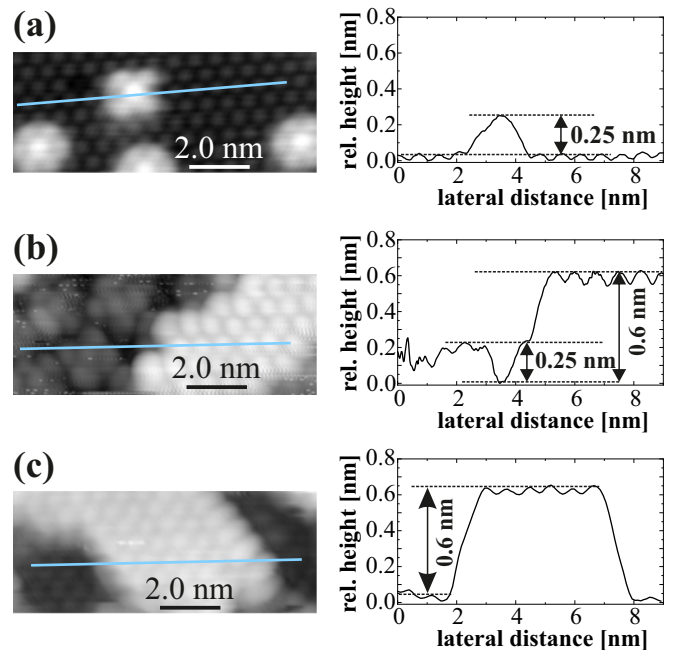


FIG. 4. Height profiles taken along the blue lines for different CoPc coverages (a) 0.2 ML CoPc ( $V_S = +2.5$  V,  $I_T = 50$  pA), (b) 1.4 ML CoPc ( $V_S = +2.5$  V,  $I_T = 20$  pA), and (c) 3.2 ML CoPc ( $V_S = +2.5$  V,  $I_T = 10$  pA).

surface and of 0.2 ML CoPc on Si:B are depicted in Fig. 5. The spectra are all taken with a photon energy of  $h\nu = 130$  eV.

For a quantitative analysis, the spectra were fitted using doublets with a spin-orbit splitting of 0.6 eV, an intensity ratio of 2:1, and Voigt line profiles for considering both lifetime and

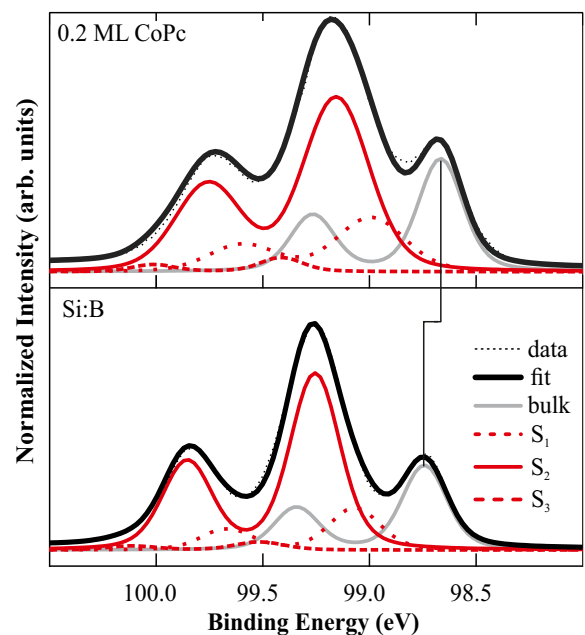


FIG. 5. Si  $2p$  core level photoemission spectra of the clean Si:B surface and of a CoPc submonolayer on the Si:B surface, recorded at a photon energy of  $h\nu = 130$  eV. The spectra are decomposed into one bulk and three surface related components ( $S_1$ ,  $S_2$ , and  $S_3$ ).

instrumental broadening. Additionally, both a constant and a Shirley-type background were used. Because of the photon energy of  $h\nu = 130$  eV, the spectra are sufficiently surface sensitive. We note that due to the high surface sensitivity it was not possible to measure meaningfully the Si  $2p$  spectra of the 3.2 ML thick CoPc film.

The spectrum of the bare and clean Si:B surface consists of one bulk component at lower binding energy and of three surface related components, labeled  $S_1$ ,  $S_2$ , and  $S_3$ , which are assigned to different surface lattice sites of the Si:B reconstruction, in agreement with other studies [35]. The used notation for the corresponding components in the Si  $2p$  core level spectra are marked in Fig. 1(b). The dominant component  $S_2$  is related to the Si adatoms as well as to the atoms bonding to these adatoms, which cannot be separated energetically.

After deposition of 0.2 ML CoPc, the Si  $2p$  spectrum can again be described by one bulk component and by three surface related components. All components are shifted by about 0.1 eV to lower binding energies as compared to the Si:B surface due to a change in band bending. Moreover, a clear change in the Gaussian width is observable for all surface related components. This broadening is an evidence that the chemical environment of the surface components has changed. The strongest change is observed for the adatom component  $S_2$ . This broadening supports the above assumption from the STM data that the  $p_z$  orbital of the Si adatom forms a hybrid state with the  $d_{z^2}$  orbital of the Co atom [19,26].

The corresponding C  $1s$  core level spectra for all measured film thicknesses (not shown here) consists of two different main features followed by two satellite features, confirming other reports on the C  $1s$  excitation [36]. No changes are observed for all studied film thicknesses, in contrast to the Si  $2p$  spectra. Consequently, the hybridization only affects the central Co atom of the molecule, while the ligand is not involved in this molecule-interface interaction. This finding is in contrast to, e.g., the doping of phthalocyanine films with K, for which the C  $1s$  PES profile is characterized by the appearance of an additional core level component [37].

For a further analysis of the electronic properties, the corresponding STS measurements were performed for the different CoPc coverages on the Si:B surface (see Fig. 6). Here the normalized differential conductivity spectra of the clean Si:B surface (gray), of the molecules at a 0.2 ML thick CoPc layer (red), and of a 3.2 ML thick CoPc film (black) are shown.

In the Si:B spectrum, an apparent band gap region of about 1.1 V with negligible conductivity is visible, corresponding to the value of the fundamental bulk band gap of Si. The gap region is bordered by the signal from of the valence and conduction band at negative and positive sample bias, respectively. At positive bias starting from about +0.5 V, a very low conductivity signal is detectable (noisy appearance of the gray curve between +0.5 V and +0.9 V). This is assigned to states from defective regions of the Si:B surface, which appear in the spectrum due to an averaging over various surface positions. Furthermore, a strong peak at +1.1 V on the conduction band side is observed corresponding to the formation of an unoccupied band of surface states [20,38,39].

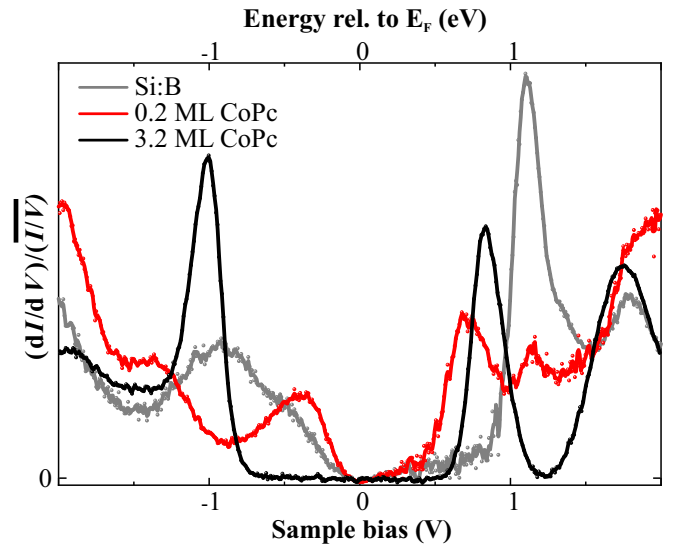


FIG. 6. STS results of the normalized differential conductivity of the bare Si:B substrate and with different CoPc coverages.

The spectrum of a 3.2 ML thick CoPc film adsorbed on the Si:B surface is depicted as a black line in Fig. 6. The spectrum is mainly characterized by a wide region without any conductivity, neighbored by two pronounced peaks, which are assigned to the highest occupied molecular orbital (HOMO, at  $-1.0$  eV) and the lowest unoccupied molecular orbital (LUMO, at  $+0.8$  eV). This assignment results in an energy gap of 1.8 eV, in agreement with the one measured in Ref. [40].

In contrast to the thick CoPc film, the LDOS spectrum of a 0.2 ML thick CoPc film, measured with the STM tip being located above the central part of the CoPc molecule (red line), shows a very different appearance: The CoPc molecule is in direct contact with the Si:B surface, resulting in a changed LDOS. A new peak appears at  $-0.4$  V at the valence band side. This occupied state is induced by a charge transfer between the Co atom and the Si:B surface resulting in a reduced electron density at the Co atom, similar to CoPc on noble metal surfaces [12,41]. From DFT calculations it is expected that a selective orbital hybridization occurs [26]. Thus, the spectral feature at lowest binding energy ( $-0.4$  V) is related to an electronic state caused by a selective orbital hybridization between the half occupied  $d_{z^2}$  orbital of the CoPc molecule and the empty  $p_z$  orbital of the Si adatom [19,26].

The STS data indicate that the interaction between the CoPc molecules and the Si:B substrate is strong and leads to additional electronic states such as the state at  $-0.4$  eV. Thus the related changes in the LDOS should also be detectable in the PES valence band measurements. In Fig. 7 the PES valence band spectra of the different CoPc coverages on the Si:B surface are shown.

Figure 7(a) shows the spectral profiles between the Fermi energy corresponding to a binding energy of 0 eV and a binding energy of about 5 eV. The gray spectrum again represents the clean Si:B surface and agrees well with the STS data: Both show a peak at about 1.0 eV and a shoulder at about

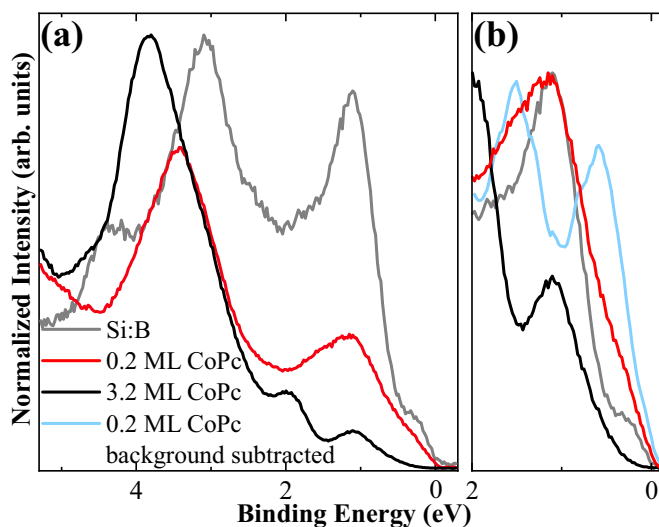


FIG. 7. (a) Valence band spectra of CoPc adsorbed on a Si:B surface with increasing film thickness, taken with a photon energy of  $h\nu = 62$  eV. (b) A close up view of the low binding energy range showing the result of the subtraction of the Si-related background from the spectrum of 0.2 ML CoPc as a light blue line (see text).

0.4 eV below the Fermi energy, as also found in Refs. [42,43]. In contrast, the spectral onset of the 3.2 ML thick CoPc film (black line) is shifted to higher binding energies, and the surface states of the clean Si:B surface are not visible any more. For the 3.2 ML thick CoPc layer the spectrum is composed of three different states. This is in very good agreement with previous photoemission measurements for CoPc on Au [12,44]. The peak at about 1.1 eV is also present in the respective STS spectrum (see Fig. 6) and assigned to the HOMO. According to results of CoPc on Au, the second state at around 2 eV is assigned to a hybrid orbital between the ligand and Co 3d states, while the broader maximum around 4 eV is assigned to a mixture of several states in this energy range [12,44]. This behavior demonstrates again that for the thick film the electronic properties resemble those of pure

CoPc, as it can be expected from the packed bundles observed in the STM images in Fig. 3.

For the 0.2 ML thick CoPc film the photoemission profile (red line) differs drastically from the other ones. Since the CoPc molecules are quite flat (1 atom thick) and only a fraction of the surface is covered, the detected electrons in PES originate mainly from the underlying and uncovered Si:B surface. In order to obtain the pure signal originating from the molecules and their interface with the Si:B surface, a fraction of the bare Si:B spectrum was subtracted from the measured one with 0.2 ML CoPc. This was done by subtracting the spectrum of the clean Si:B surface after the 0.2 ML spectrum was normalized with respect to different states from the clean Si:B surface. The result of this subtraction is depicted in Fig. 7(b) by the light blue line. This spectrum shows a first maximum at a binding energy of 0.4 eV followed by a second peak at about 1.4 eV, being in nice agreement with the STS data (Fig. 6).

#### IV. SUMMARY

To summarize, the scanning tunneling microscopy and spectroscopy as well as the photoemission results show that for the submonolayer of CoPc on the clean Si:B surface a charge transfer occurs between the substrate and the central Co atom of the flat-lying molecules. Our data demonstrate that this charge transfer does not affect the ligand of the molecule. We assign this behavior to a hybrid state between the Co and Si orbitals. For higher CoPc coverages on Si:B surfaces a reordering of the film structure towards ordered molecular domains with a tilted configuration occurs, resulting in a strongly reduced interaction with the substrate, but in electronic properties as known for pure CoPc.

#### ACKNOWLEDGMENTS

The authors like to thank K. Horn and Ch. Papp for providing the ARPES chamber. J. Döhring is acknowledged for technical support and BESSY II (Helmholtz-Zentrum Berlin) for providing the beamtimes. Financial support by the Deutsche Forschungsgemeinschaft, Project No. LI 3068/2-1 is gratefully acknowledged.

- [1] N. R. Armstrong, W. Wang, D. M. Alloway, D. Placencia, E. Ratcliff, and M. Brumbach, *Macromol. Rapid Commun.* **30**, 717 (2009).
- [2] P. Peumans and S. R. Forrest, *Appl. Phys. Lett.* **79**, 126 (2001).
- [3] B. P. Rand, J. Genoe, P. Heremans, and J. Poortmans, *Prog. Photovolt.* **15**, 659 (2007).
- [4] Z. Bao, A. J. Lovinger, and A. Dodabalapur, *Appl. Phys. Lett.* **69**, 3066 (1996).
- [5] V. Dediu, M. Murgia, F. C. Matocotta, C. Taliani, and S. Barbanera, *Solid State Commun.* **122**, 181 (2002).
- [6] W. J. M. Naber, S. Faez, and W. G. v. d. Wiel, *J. Phys. D: Appl. Phys.* **40**, R205 (2007).
- [7] A. Zhao, Q. Li, L. Chen, H. Xiang, W. Wang, S. Pan, B. Wang, X. Xiao, J. Yang, J. G. Hou, and Q. Zhu, *Science* **309**, 1542 (2005).
- [8] J. D. Baran, J. A. Larsson, R. A. J. Woolley, Y. Cong, P. J. Moriarty, A. A. Cafolla, K. Schulte, and V. R. Dhanak, *Phys. Rev. B* **81**, 075413 (2010).
- [9] F. Petraki, H. Peisert, F. Lattayer, U. Aygül, A. Vollmer, and T. Chassé, *J. Phys. Chem. C* **115**, 21334 (2011).
- [10] E. Annesse, J. Fujii, I. Vobornik, and G. Rossi, *J. Phys. Chem. C* **115**, 17409 (2011).
- [11] P. Gargiani, M. Angelucci, C. Mariani, and M. G. Betti, *Phys. Rev. B* **81**, 085412 (2010).
- [12] S. Lindner, U. Treske, M. Grobosch, and M. Knupfer, *Appl. Phys. A* **105**, 921 (2011).
- [13] H. Yamane and N. Kosugi, *J. Phys. Chem. C* **120**, 24307 (2016).
- [14] P. Dumas, F. Thibaudau, and F. Salvan, *J. Microsc.* **152**, 751 (1988).

- [15] F. Thibaudau, P. Dumas, P. Mathiez, A. Humbert, D. Satti, and F. Salvan, *Surf. Sci.* **211-212**, 148 (1989).
- [16] P. Bedrossian, R. D. Meade, K. Mortensen, D. M. Chen, J. A. Golovchenko, and D. Vanderbilt, *Phys. Rev. Lett.* **63**, 1257 (1989).
- [17] E. Kaxiras, K. C. Pandey, F. J. Himpsel, and R. M. Tromp, *Phys. Rev. B* **41**, 1262 (1990).
- [18] H. Q. Shi, M. W. Radny, and P. V. Smith, *Phys. Rev. B* **66**, 085329 (2002).
- [19] S. R. Wagner, B. Huang, C. Park, J. Feng, M. Yoon, and P. Zhang, *Phys. Rev. Lett.* **115**, 096101 (2015).
- [20] A. Tan, S. R. Wagner, and P. P. Zhang, *Phys. Rev. B* **96**, 035313 (2017).
- [21] R. M. Feenstra, J. A. Stroscio, J. Tersoff, and A. P. Fein, *Phys. Rev. Lett.* **58**, 1192 (1987).
- [22] R. Feenstra, J. A. Stroscio, and A. Fein, *Surf. Sci.* **181**, 295 (1987).
- [23] M. Prietsch, A. Samsavar, and R. Ludeke, *Phys. Rev. B* **43**, 11850 (1991).
- [24] H. Eisele, S. Borisova, L. Ivanova, M. Dähne, and P. Ebert, *J. Vac. Sci. Technol. B* **28**, C5G11 (2010).
- [25] X. Lu, K. W. Hipps, X. D. Wang, and U. Mazur, *J. Am. Chem. Soc.* **118**, 7197 (1996).
- [26] R. G. A. Veiga, R. H. Miwa, and A. B. McLean, *Phys. Rev. B* **93**, 115301 (2016).
- [27] I. Kröger, B. Stadtmüller, C. Stadler, J. Ziroff, M. Kochler, A. Stahl, F. Pollinger, T.-L. Lee, J. Zegenhagen, F. Reinert, and C. Kumpf, *New J. Phys.* **12**, 083038 (2010).
- [28] M. G. Betti, P. Gargiani, R. Frisenda, R. Biagi, A. Cossaro, A. Verdini, L. Floreano, and C. Mariani, *J. Phys. Chem. C* **114**, 21638 (2010).
- [29] L. Massimi, M. Angelucci, P. Gargiani, M. G. Betti, S. Montoro, and C. Mariani, *J. Chem. Phys.* **140**, 244704 (2014).
- [30] Y. Wang, J. Kröger, R. Berndt, and H. Tang, *J. Am. Chem. Soc.* **132**, 12546 (2010).
- [31] S. R. Wagner, R. R. Lunt, and P. Zhang, *Phys. Rev. Lett.* **110**, 086107 (2013).
- [32] F. Bartolomé, O. Bunău, L. M. García, C. R. Natoli, M. Piantek, J. I. Pascual, I. K. Schuller, T. Gredig, F. Wilhelm, A. Rogalev, and J. Bartolomé, *J. Appl. Phys.* **117**, 17A735 (2015).
- [33] M.-L. Tao, Y.-B. Tu, K. Sun, Y. Zhang, X. Zhang, Z.-B. Li, S.-J. Hao, H.-F. Xiao, J. Ye, and J.-Z. Wang, *J. Phys. D: Appl. Phys.* **49**, 015307 (2015).
- [34] K. Sun, M.-L. Tao, Y.-B. Tu, and J.-Z. Wang, *Molecules* **22**, 740 (2017).
- [35] T. M. Grehk, M. Göthelid, U. O. Karlsson, L. S. O. Johansson, S. M. Gray, and K. O. Magnusson, *Phys. Rev. B* **52**, 11165 (1995).
- [36] M. Grobosch, C. Schmidt, R. Kraus, and M. Knupfer, *Org. Electron.* **11**, 1483 (2010).
- [37] V. Aristov, O. Molodtsova, and M. Knupfer, *Org. Electron.* **12**, 372 (2011).
- [38] Y. Makoudi, J. Jeannoutot, F. Palmino, F. Chérioux, G. Copie, C. Krzeminski, F. Cleri, and B. Grandidier, *Surf. Sci. Rep.* **72**, 316 (2017).
- [39] T. M. Grehk, P. Mårtensson, and J. M. Nicholls, *Phys. Rev. B* **46**, 2357 (1992).
- [40] M. Takada and H. Tada, *Jpn. J. Appl. Phys.* **44**, 5332 (2005).
- [41] F. Petraki, H. Peisert, I. Biswas, and T. Chassé, *J. Phys. Chem. C* **114**, 17638 (2010).
- [42] J. Krügener, H. J. Osten, and A. Fissel, *Phys. Rev. B* **83**, 205303 (2011).
- [43] S. Menzli, A. Laribi, H. Mrezguia, I. Arbi, A. Akremi, C. Chefi, F. Chérioux, and F. Palmino, *Surf. Sci.* **654**, 39 (2016).
- [44] M. Grobosch, V. Y. Aristov, O. V. Molodtsova, C. Schmidt, B. P. Doyle, S. Nannarone, and M. Knupfer, *J. Phys. Chem. C* **113**, 13219 (2009).